Mitigation of Loopback Self-Interference in Full-Duplex MIMO Relays

Taneli Riihonen, *Student Member, IEEE*, Stefan Werner, *Senior Member, IEEE*, and Risto Wichman

***Abstract*—Full-duplex relaying is more spectrally efficient than half-duplex relaying as only one channel use is needed per two hops. However, it is crucial to minimize relay self-interference to render full duplex feasible. For this purpose, we analyze a broad range of multiple-input multiple-output (MIMO) mitigation schemes: natural isolation, time-domain cancellation, and spatial suppression. Cancellation subtracts replicated interference signal from the relay input while suppression reserves spatial dimensions for receive and transmit filtering. Spatial suppression can be achieved by antenna subset selection, null-space projection, i.e., receiving and transmitting in orthogonal subspaces, or joint transmit and receive beam selection to support more spatial streams by choosing the minimum eigenmodes for overlapping subspaces. In addition, minimum mean square error (MMSE) filtering can be employed to maintain the desired signal quality, which is inherent for cancellation, and the combination of time- and spatial-domain processing may be better than either alone. Targeting at minimal interference power, we solve optimal filters for each scheme in the cases of joint, separate and independent design. The performance of mitigation schemes is evaluated and compared by simulations. The results confirm that self-interference can be mitigated effectively also in the presence of imperfect side information.**

***Index Terms*—Amplify-and-forward (AF), antenna selection (AS), beam selection (BS), decode-and-forward (DF), full-duplex, interference cancellation, multiple-input multiple-output (MIMO) relay, minimum mean square error (MMSE), null-space projection, self-interference.**

I. Introduction

RELAYING, i.e., multihop communication, is a promising technique to provide lower transmit powers, higher throughput and more extensive coverage in future wireless systems. Likewise, single-hop multiple-input multiple-output (MIMO) transmission has attracted wide research interest, and emerging wireless systems utilize extensively MIMO techniques such as spatial division multiplexing. Hence, if relays are used, they need to be equipped with antenna arrays as well to avoid a key-hole effect, i.e., squashing multiple spatial streams through a rank-one device. This paper focuses on the combination of MIMO and relaying techniques and develops new baseband signal processing techniques to improve spectral efficiency.

An essential classification of relaying techniques is between *full-duplex* and *half-duplex* operation modes. In fact, the choice of the operation mode is a fundamental tradeoff between spectral efficiency and self-interference. A full-duplex relay receives and transmits at the same time on the same channel. Hence, spectrum resources are utilized efficiently but as a downside the relay is subject to *loop interference* (LI) due to signal leakage from the relay's transmission to its own reception. The earlier literature often pessimistically sees this self-interference as an insurmountable problem, and resorts to the half-duplex mode by allocating separate time slots or frequency bands for relay reception and transmission. This is a simple way to avoid interference by splurging spectrum.

This paper concentrates on the main *open* technical problem in full-duplex relaying: *How to mitigate the loop interference efficiently?* For investigating and comparing several solutions, our main motivation is to improve the spectral efficiency of relay systems by avoiding the need of two channel uses for one end-to-end transmission that is inherent for half-duplex relays. Throughout the paper, the *mitigation* schemes are categorized into three subtypes: A) natural *isolation*, B) time-domain *cancellation*, and C) spatial *suppression*. Consequently, we aim at showing that the loop interference can be mitigated sufficiently and, thus, the full-duplex mode becomes a feasible and viable alternative for the half-duplex mode.

A. Related Literature

The literature on MIMO relaying can be classified as follows based on how the self-interference problem is treated:

1) Most earlier papers, e.g., [1]–[11], consider half-duplex relaying in which *the loop interference is inherently avoided*. Some papers, e.g., [1]–[6], develop half-duplex protocols for the case in which *the direct source-destination link is blocked*. Our results are directly applicable for the full-duplex counterparts of these systems and enable more spectrally-efficient implementation once the loop interference is appropriately mitigated. The other papers, e.g., [7]–[11], *exploit the direct link* as an extra diversity branch. The direct link is orthogonal by design in the half-duplex mode whereas the destination receives superposition of the direct and relayed transmissions in the full-duplex mode. Also for these systems, the full-duplex counterparts are feasible with proper signal separation in the destination.

Manuscript received April 12, 2010; revised April 05, 2011, July 15, 2011; accepted July 21, 2011. Date of publication August 15, 2011; date of current version November 16, 2011. The associate editor coordinating the review of this manuscript and approving it for publication was Prof. Yimin Zhang. This work was partially supported by the Centre of Excellence in Smart Radios and Wireless Research (SMARAD) and by the Academy of Finland.

The authors are with the Department of Signal Processing and Acoustics, Aalto University School of Electrical Engineering, FI-00076 Aalto, Finland (e-mail: taneli.riihonen@aalto.fi; stefan.werner@aalto.fi; risto.wichman@aalto.fi).

Color versions of one or more of the figures in this paper are available online at http://ieeexplore.ieee.org.

Digital Object Identifier 10.1109/TSP.2011.2164910

2) Some information theory-oriented papers, e.g., [10]–[19], study various full-duplex relaying schemes *without considering the deleterious effect of the loop interference* albeit otherwise presenting many seminal contributions. In particular, these papers tend to provide minimal (if any at all) explanations and references for the mitigation of the loop interference. Our results will support this body of literature by providing validation and a retroactive reference for a central baseline assumption not verified in detail before.
3) The smallest group of earlier papers *accounts explicitly for the effect of the loop interference* in full-duplex relaying. The early results consider exclusively single-input single-output (SISO) repeaters, see, e.g., [20]–[23]. For *full-duplex MIMO relays with loop interference*, our literature search elicited preliminary ideas [24], [25] and recent studies [26]–[31] conducted in parallel with our work reported first in [32]. These papers tackle the problem of loop interference mitigation in a limited scope, e.g., restricting the system to support only one spatial stream or providing suboptimal solutions. Moreover, the relay processing delay is neglected in [28]–[30], which, as discussed in [32], renders the relay practically impossible to implement or makes the loop interference not harmful. Reference [31] studies loop channel estimation in full-duplex MIMO relays and, thus, supports our analysis which starts presuming that such side information is already made available.

Analog SISO repeaters have been employed for a long time in cellular networks. Instead, we consider modern, sophisticated, digital relays that are capable of baseband signal processing, and, in particular, employ multiantenna techniques. Some prototypes of full-duplex MIMO relays have already been developed, see, e.g., [33] and [34]. After mitigating the loop interference as shown herein, they become a viable solution to transparently boost the coverage of future cellular systems.

B. Contributions and Organization of the Paper

This paper contributes to the study of full-duplex MIMO relays as follows:[1]

- In Section II, we set up a generic system model that explicitly accounts for the loop interference, the relay processing delay, and the imperfections of the side information exploited in the mitigation of loop interference. These specifics are important but omitted in some papers.
- In Section III-A, we summarize the reference schemes: Natural isolation (Section III-A1), that is needed in order to avoid relay receiver saturation, and digital MIMO time-domain cancellation (Section III-A2), which generalizes the schemes used in SISO repeaters.
- In Section III-B, we propose and analyze *novel* spatial suppression schemes based on antenna selection (Section III-B1), beam selection (Section III-B2), null-space projection (Section III-B3), and minimum mean square error (MMSE) filters (Section III-B4). For every scheme, we specify explicitly the minimization of the self-interference as the optimization target and provide general solutions for the optimal filters. Examples 1–4 show why [25]–[28] present only simplified or suboptimal special cases for some of our general schemes and why their schemes are applicable only in specific system setups.
- In Section III-B5, we introduce the combination of time-domain cancellation and spatial suppression for reducing the effect of imperfect side information in mitigation.
- In Section IV, the mitigation schemes are compared extensively with simulations on bit-error rate and isolation improvement. The results verify that the loop interference can be mitigated significantly or even eliminated completely in the ideal case, but, in practice, there will be some weak residual interference due to imperfect side information used for mitigation.

The remainder of the paper is also outlined above.

C. Nomenclature

We let $\mathbf{X}^T$, $\mathbf{X}^H$, $\mathbf{X}^{-1}$, $\mathbf{X}^+$, $\mathrm{rk}\{\mathbf{X}\}$, $\mathrm{tr}\{\mathbf{X}\}$, and $\|\mathbf{X}\|_F = \sqrt{\mathrm{tr}\{\mathbf{X}\mathbf{X}^H\}}$ denote the transpose, conjugate transpose, inverse, Moore-Penrose pseudoinverse, rank, trace, and Frobenius norm of matrix $\mathbf{X}$, respectively. The Euclidean norm of vector $\mathbf{x}$ is given by $\|\mathbf{x}\|_2 = \sqrt{\mathbf{x}^H\mathbf{x}}$, and $\binom{N}{\hat{N}}$ is the binomial coefficient, i.e., the number of combinations to choose $\hat{N}$ elements from a set of N elements. Respective column and row subset selection matrices of appropriate dimensions are represented by $\mathbf{S}$ and $\mathbf{S}^T$ which are binary matrices such that $\sum_i \{\mathbf{S}\}_{i,j} = 1$ for all j and $\sum_j \{\mathbf{S}\}_{i,j} \in \{0,1\}$ for all i. Identity and zero matrices of appropriate dimensions are $\mathbf{I}$ and $\mathbf{0}$, respectively. The expectation operator is denoted by $\mathcal{E}\{\cdot\}$.

II. System Model

Let us consider the generic wireless multihop network illustrated in the upper left corner of Fig. 1. The network comprises nodes operating in both half-duplex and full-duplex modes and it is not restricted to any specific multihop routing protocol or multiple access strategy for the simultaneous transmissions. We then focus on two-hop communication through any full-duplex relay (R) node from a set of source (S) nodes to a set of destination (D) nodes as illustrated in the lower right corner of Fig. 1. The full-duplex relay receives and transmits simultaneously on the same frequency which necessitates to model explicitly the resulting loop interference (LI) signal.

The sources and the destinations have in total N_{S} transmit and N_{D} receive antennas, respectively, and the relay is equipped with N_{rx} receive and N_{tx} transmit antennas. Before applying mitigation techniques the relay is likely implemented with spatially separated receive and transmit antenna arrays which constitutes natural isolation (see Section III-A1). However, the following results are also applicable in full-duplex relaying with a single antenna array which is optimistically considered in [26]. We set $N_{\mathrm{rx}} = N_{\mathrm{tx}}$ in this special case.

A. Signal Model

The signal model is built upon frequency-flat block-fading channels as in the majority of related papers, see, e.g., [1]–[19], [25], [26], [28]–[30]. This implies that the system exploits

[1]A part of these results has been preliminarily presented in conference paper [32]. For the current paper, the material has been essentially rewritten and extended: the system model is improved, novel mitigation schemes are introduced, the analysis is more thorough, and all simulation results are new.

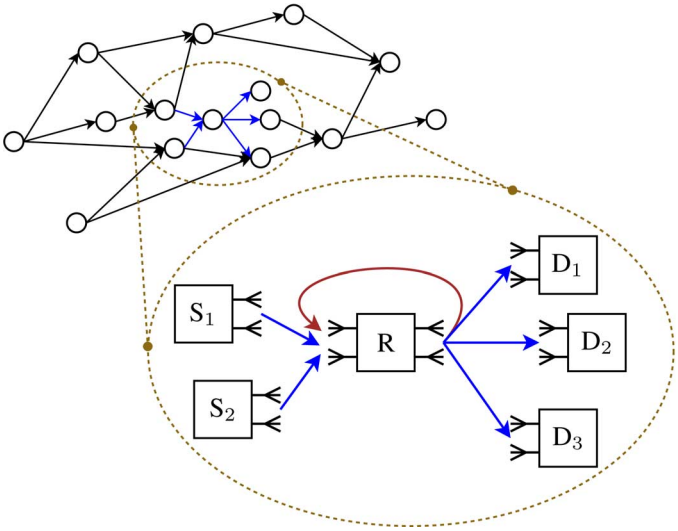

Fig. 1. A wireless multihop network containing a full-duplex relay subject to loop interference.

orthogonal frequency division multiplexing (OFDM) for broadband transmission over multipath channels, and the signal model represents a single narrowband subcarrier.

For time instant i, let matrices $\mathbf{H}_{\mathrm{SR}}[i] \in \mathbb{C}^{N_{\mathrm{rx}} \times N_{\mathrm{S}}}$, $\mathbf{H}_{\mathrm{LI}}[i] \in \mathbb{C}^{N_{\mathrm{rx}} \times N_{\mathrm{tx}}}$, and $\mathbf{H}_{\mathrm{RD}}[i] \in \mathbb{C}^{N_{\mathrm{D}} \times N_{\mathrm{tx}}}$ represent the respective MIMO channels from all sources to the relay, from the relay output to the relay input, and from the relay to all destinations. The sources transmit the combined signal vector $\mathbf{x}[i] \in \mathbb{C}^{N_{\mathrm{S}} \times 1}$, and the relay transmits signal vector $\mathbf{t}[i] \in \mathbb{C}^{N_{\mathrm{tx}} \times 1}$ while it simultaneously receives signal vector $\mathbf{r}[i] \in \mathbb{C}^{N_{\mathrm{rx}} \times 1}$. This creates a feedback loop from the relay output to the relay input through channel $\mathbf{H}_{\mathrm{LI}}[i]$.

The relaying protocol is denoted by the generic function

$$\mathbf{t}[i] = f(\mathbf{r}[i-\tau], \mathbf{r}[i-(\tau+1)], \mathbf{r}[i-(\tau+2)], \ldots) \quad (1)$$

which generates an output sample based on the sequence of input samples and causes integer processing delay $\tau > 0$. We focus on the mitigation of the loop interference and, thereby, keep the proposed schemes transparent and applicable with most of the readily available relaying protocols.

Remark 1: The processing delay is strictly positive because we consider wideband transmission over multipath channels in contrast to [28]–[30]. In particular, omitting the delay causes severe causality problems in the practical implementation of relaying protocols: It is impossible to process a subcarrier and retransmit the OFDM symbol before the respective OFDM symbol is first completely received and demodulated. Furthermore, the loop signal may not be harmful at all with zero processing delay because the relay transmission only amplifies the same input signal. See [32] for more discussion on the consequences of neglecting the processing delay.

Finally, the respective received signals in the relay and in the destinations can be expressed as

$$\begin{aligned} \mathbf{r}[i] &= \mathbf{H}_{\mathrm{SR}}[i]\,\mathbf{x}[i] + \mathbf{H}_{\mathrm{LI}}[i]\,\mathbf{t}[i] + \mathbf{n}_{\mathrm{R}}[i], \\ \mathbf{y}[i] &= \mathbf{H}_{\mathrm{RD}}[i]\,\mathbf{t}[i] + \mathbf{n}_{\mathrm{D}}[i] \end{aligned} \quad (2)$$

where $\mathbf{n}_{\mathrm{R}}[i] \in \mathbb{C}^{N_{\mathrm{rx}} \times 1}$ and $\mathbf{n}_{\mathrm{D}}[i] \in \mathbb{C}^{N_{\mathrm{D}} \times 1}$ are additive noise vectors in the relay and in the destinations, respectively. All signal and noise vectors have zero mean. Signal and noise covariance matrices are denoted by $\mathbf{R}_{\mathbf{x}} = \mathcal{E}\{\mathbf{x}[i]\mathbf{x}^H[i]\}$, $\mathbf{R}_{\mathbf{t}} = \mathcal{E}\{\mathbf{t}[i]\mathbf{t}^H[i]\}$, and $\mathbf{R}_{\mathbf{n}_{\mathrm{R}}} = \mathcal{E}\{\mathbf{n}_{\mathrm{R}}[i]\mathbf{n}_{\mathrm{R}}^H[i]\}$. For clarity, we will omit the time indices in the rest of the paper.

B. Side Information for Mitigation Techniques

We consider mitigation techniques that can be implemented transparently, i.e., using only information that the relay is expected to know by design or is able to measure by itself. In other words, mitigation may exploit knowledge of only $\mathbf{t}$, $\mathbf{H}_{\mathrm{LI}}$, and $\mathbf{H}_{\mathrm{SR}}$. However, we assume that the available side information is degraded due to the following non-idealities which manifest themselves in the form of noise. In this paper, the noise is assumed to be completely unknown for the mitigation schemes while some additional information such as the covariance or norm bounds of the errors could facilitate a "robust" approach.

1) Channel Estimation Noise: The relay may exploit any off-the-shelf technique or one of the schemes developed specifically for full-duplex relays [23], [31] to obtain the respective estimates $\tilde{\mathbf{H}}_{\mathrm{LI}}$ and $\tilde{\mathbf{H}}_{\mathrm{SR}}$ of $\mathbf{H}_{\mathrm{LI}}$ and $\mathbf{H}_{\mathrm{SR}}$. We model the practically non-ideal estimation process by defining estimation noises $\Delta\tilde{\mathbf{H}}_{\mathrm{LI}}$ and $\Delta\tilde{\mathbf{H}}_{\mathrm{SR}}$ such that the estimates differ from the true channel values:

$$\mathbf{H}_{\mathrm{LI}} = \tilde{\mathbf{H}}_{\mathrm{LI}} + \Delta\tilde{\mathbf{H}}_{\mathrm{LI}} \text{ and } \mathbf{H}_{\mathrm{SR}} = \tilde{\mathbf{H}}_{\mathrm{SR}} + \Delta\tilde{\mathbf{H}}_{\mathrm{SR}}. \quad (3)$$

All elements of $\Delta\tilde{\mathbf{H}}_{\mathrm{LI}}$ and $\Delta\tilde{\mathbf{H}}_{\mathrm{SR}}$ are assumed to be independent (both mutually and from the corresponding channels) circularly symmetric complex Gaussian random variables. The variance of the estimation noise is defined by relative estimation error $\epsilon_{\mathbf{H}}$ such that

$$\mathcal{E}\{|\{\Delta\tilde{\mathbf{H}}_{\mathrm{LI}}\}_{i,j}|^2\} = \epsilon_{\mathbf{H}}^2 \mathcal{E}\{|\{\mathbf{H}_{\mathrm{LI}}\}_{i,j}|^2\} \quad (4)$$

for all i, j. Analogous relation holds between $\Delta\tilde{\mathbf{H}}_{\mathrm{SR}}$ and $\mathbf{H}_{\mathrm{SR}}$.

2) Transmit Signal Noise: The relay knows perfectly the digital baseband signal $\tilde{\mathbf{t}}$ it generates, but the actual transmitted signal $\mathbf{t}$ cannot be exactly known. This is because any practical implementation of conversion between baseband and radio frequency is prone to various distortion effects such as carrier frequency offset, oscillator phase noise, AD/DA conversion imperfections, I/Q imbalance, and power amplifier nonlinearity among others. We model the joint effect of all imperfections by introducing additive transmit distortion noise $\Delta\tilde{\mathbf{t}}$ such that

$$\mathbf{t} = \tilde{\mathbf{t}} + \Delta\tilde{\mathbf{t}}. \quad (5)$$

Furthermore, we model all elements of $\Delta\tilde{\mathbf{t}}$ with independent zero-mean random variables, and define their variance with relative distortion $\epsilon_{\mathbf{t}}$. The covariance matrix of the transmit noise becomes

$$\mathbf{R}_{\Delta\tilde{\mathbf{t}}} = \epsilon_{\mathbf{t}}^2 \frac{\mathrm{tr}\,\{\mathbf{R}_{\tilde{\mathbf{t}}}\}}{N_{\mathrm{tx}}} \mathbf{I}. \quad (6)$$

We assume that $\tilde{\mathbf{t}}$ and $\Delta\tilde{\mathbf{t}}$ are uncorrelated which implies that $\mathbf{R}_{\mathbf{t}} = \mathbf{R}_{\tilde{\mathbf{t}}} + \mathbf{R}_{\Delta\tilde{\mathbf{t}}}$ in which $\mathbf{R}_{\tilde{\mathbf{t}}} = \mathcal{E}\{\tilde{\mathbf{t}}\tilde{\mathbf{t}}^H\}$.

III. Mitigation of Loop Interference

In what follows, we decouple the mitigation of loop interference from the design of the relaying protocol and develop solutions that transform the $N_{\rm rx} \times N_{\rm tx}$ relay to an equivalent "interference-free" $\hat{N}_{\rm rx} \times \hat{N}_{\rm tx}$ relay. Here $\hat{N}_{\rm rx} \leq N_{\rm rx}$ and $\hat{N}_{\rm tx} \leq N_{\rm tx}$ represent the input and output dimensions (or the number of spatial streams) reserved for the relaying protocol.

The target is to make residual loop interference so infinitesimal that it can be regarded simply as additional relay input noise. Thus, we transform the signal model from (2) to

$$\hat{\mathbf{r}} = \hat{\mathbf{H}}_{\rm SR}\mathbf{x} + \hat{\mathbf{n}}_{\rm R}, \quad \mathbf{y} = \hat{\mathbf{H}}_{\rm RD}\hat{\mathbf{t}} + \mathbf{n}_{\rm D} \tag{7}$$

where $\hat{\mathbf{r}} \in \mathbb{C}^{\hat{N}_{\rm rx}\times 1}$ and $\hat{\mathbf{t}} \in \mathbb{C}^{\hat{N}_{\rm tx}\times 1}$ are the respective receive and transmit signal vectors of the equivalent interference-free relay, $\hat{\mathbf{H}}_{\rm SR} \in \mathbb{C}^{\hat{N}_{\rm rx}\times N_{\rm S}}$ and $\hat{\mathbf{H}}_{\rm RD} \in \mathbb{C}^{N_{\rm D}\times \hat{N}_{\rm tx}}$ represent the respective equivalent MIMO channels from all sources to the interference-free relay and from the interference-free relay to all destinations, and $\hat{\mathbf{n}}_{\rm R} \in \mathbb{C}^{\hat{N}_{\rm rx}\times 1}$ is the equivalent receiver noise vector including all residual loop interference after mitigation. The covariance matrix of $\hat{\mathbf{t}}$ is $\mathbf{R}_{\hat{\mathbf{t}}} = \mathcal{E}\{\hat{\mathbf{t}}\hat{\mathbf{t}}^H\}$.

Remark 2: The equivalent "interference-free" relay applies relaying protocol $\hat{f}(\cdot)$ to obtain $\hat{\mathbf{t}}$ from $\hat{\mathbf{r}}$ according to (1). By decoupling the mitigation from the protocol, the relay may adopt, directly or after minor modifications, any of the protocols designed for cases without loop interference in [1]–[19]. However, the system setup or the relaying protocol may still affect the choice of $\hat{N}_{\rm rx}$ and $\hat{N}_{\rm tx}$.

A. Reference Mitigation Schemes

1) Natural Isolation: The relay installation should guarantee some *natural* isolation (represented by $\mathbf{H}_{\rm LI}$) to facilitate the usage of signal processing techniques which provide additional *man-made* isolation. This is because, in practice, the dynamic range of the relay receiver circuitry is limited, and, thus, large difference in power levels may saturate the receiver rendering any attempt to recover the desired signal futile.

With separated receive and transmit antenna arrays, natural isolation arises from the sheer *physical distance between the arrays*, and rational installation guarantees obstacles in between the arrays to block the line-of-sight. For this purpose, the installation may exploit surrounding buildings or add a shielding plate [22]. Furthermore, *antenna elements can be directional* and pointed at opposite directions [20], [22], and their polarizations may be orthogonal. If the same antenna array is used for both receiving and transmitting as in [26], all natural isolation comes solely from the *duplexer* connecting the input and output feeds to the same physical antenna element. However, isolation offered even by the most high-end duplexers may not be sufficient for communication.

Exploiting the signal model from (2), the mean square error (MSE) matrix of the relay input signal is given by

$$\begin{aligned}\mathbf{M} &= \mathcal{E}\left\{\left(\mathbf{H}_{\rm SR}\mathbf{x} + \mathbf{n}_{\rm R} - \mathbf{r}\right)\left(\mathbf{H}_{\rm SR}\mathbf{x} + \mathbf{n}_{\rm R} - \mathbf{r}\right)^H\right\} \\ &= \mathcal{E}\left\{\mathbf{H}_{\rm LI}\mathbf{t}\mathbf{t}^H\mathbf{H}_{\rm LI}^H\right\} = \mathbf{H}_{\rm LI}\mathbf{R}_{\mathbf{t}}\mathbf{H}_{\rm LI}^H,\end{aligned} \tag{8}$$

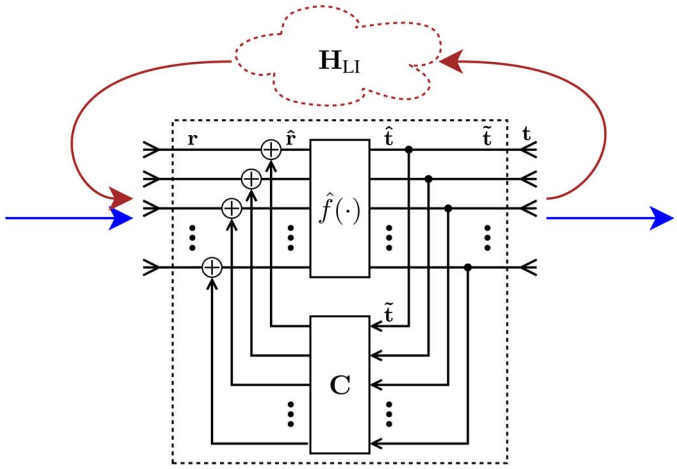

Fig. 2. Time-domain loop interference cancellation in a full-duplex MIMO relay by subtracting an estimate of the loop signal.

which yields the loop interference power as

$$P_{\rm I} = {\rm tr}\{\mathbf{M}\} = \mathcal{E}\left\{{\rm tr}\left\{\mathbf{H}_{\rm LI}\mathbf{t}\mathbf{t}^H\mathbf{H}_{\rm LI}^H\right\}\right\} = \mathcal{E}\left\{\|\mathbf{H}_{\rm LI}\mathbf{t}\|_2^2\right\}. \tag{9}$$

In the following, we presume that all means of improving natural isolation have been first exploited and then concentrate on signal processing techniques to mitigate the residual interference, i.e., the effect of $\mathbf{H}_{\rm LI} \neq \mathbf{0}$. Measurements show that natural isolation is not often sufficient alone [20], [22], [34]. Hence, our study excludes the exceptional setups in which natural isolation is large without any additional mitigation, e.g., a relay with the receive array placed outdoors and the transmit array providing underground coverage in a tunnel.

2) Time-Domain Cancellation (TDC): Cancellation is based on the reasonable presumption that the relay always knows its own transmitted signal at least approximately. If the relay can also determine the loop channel, the interference signal may be replicated and removed from the received signal. In practice, the relay may apply conventional *analog precancellation* to improve the feasibility of the digital mitigation techniques for lower dynamic range. However, the implementation of the electronics becomes expensive and difficult if the respective circuit is more sophisticated than a phase shifter that removes one (ideally the strongest) multipath component.

The considered TDC scheme is a straightforward MIMO extension for earlier SISO schemes [21]–[23], implemented as illustrated in Fig. 2 (similar structures are used in [28]–[32]): The relay contains a feedback loop with MIMO cancellation filter $\mathbf{C} \in \mathbb{C}^{N_{\rm rx}\times N_{\rm tx}}$. Thus, (2), (5), and (7) can be related as $\hat{\mathbf{r}} = \mathbf{r} + \mathbf{C}\tilde{\mathbf{t}}$, $\tilde{\mathbf{t}} = \hat{\mathbf{t}}$, $\mathbf{R}_{\tilde{\mathbf{t}}} = \mathbf{R}_{\hat{\mathbf{t}}}$, $\hat{\mathbf{H}}_{\rm SR} = \mathbf{H}_{\rm SR}$, and $\hat{\mathbf{H}}_{\rm RD} = \mathbf{H}_{\rm RD}$.

The equivalent receiver noise vector of the "interference-free" relay becomes

$$\hat{\mathbf{n}}_{\rm R} = \hat{\mathbf{H}}_{\rm LI}\hat{\mathbf{t}} + \mathbf{H}_{\rm LI}\boldsymbol{\Delta}\tilde{\mathbf{t}} + \mathbf{n}_{\rm R} \tag{10}$$

in which the residual loop interference channel is

$$\hat{\mathbf{H}}_{\rm LI} = \mathbf{H}_{\rm LI} + \mathbf{C} = \tilde{\mathbf{H}}_{\rm LI} + \mathbf{C} + \boldsymbol{\Delta}\tilde{\mathbf{H}}_{\rm LI}. \tag{11}$$

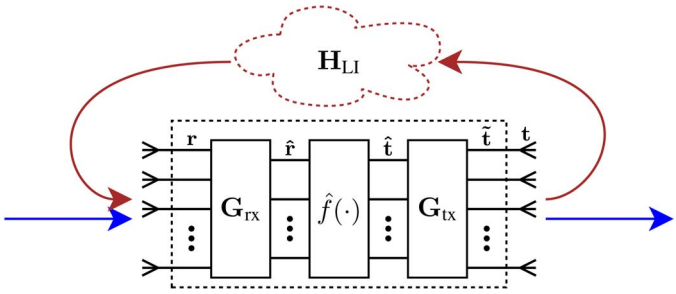

Fig. 3. Spatial loop interference suppression in a full-duplex MIMO relay by using linear receive and transmit filters.

The MSE matrix of the relay input signal becomes

$$\begin{aligned}\mathbf{M} &= \mathcal{E}\left\{(\mathbf{H}_{\mathrm{SR}}\mathbf{x}+\mathbf{n}_{\mathrm{R}}-\hat{\mathbf{r}})(\mathbf{H}_{\mathrm{SR}}\mathbf{x}+\mathbf{n}_{\mathrm{R}}-\hat{\mathbf{r}})^H\right\} \\ &= (\mathbf{H}_{\mathrm{LI}}+\mathbf{C})\mathbf{R}_{\hat{\mathbf{t}}}(\mathbf{H}_{\mathrm{LI}}+\mathbf{C})^H + \mathbf{H}_{\mathrm{LI}}\mathbf{R}_{\Delta\tilde{\mathbf{t}}}\mathbf{H}_{\mathrm{LI}}^H. \quad (12)\end{aligned}$$

The first term includes the channel estimation error and the second term arises due to the transmit signal noise. Cancellation can only minimize the known part of the first term by choosing $\mathbf{C} = -\hat{\mathbf{H}}_{\mathrm{LI}}$ which results in $\hat{\mathbf{H}}_{\mathrm{LI}} = \Delta\tilde{\mathbf{H}}_{\mathrm{LI}}$. Thereby, (12) yields the residual interference power as

$$\begin{aligned}P_{\mathrm{I}} &= \mathrm{tr}\{\mathbf{M}\} = \mathrm{tr}\left\{\Delta\tilde{\mathbf{H}}_{\mathrm{LI}}\mathbf{R}_{\hat{\mathbf{t}}}\Delta\tilde{\mathbf{H}}_{\mathrm{LI}}^H\right\} + \mathrm{tr}\left\{\mathbf{H}_{\mathrm{LI}}\mathbf{R}_{\Delta\tilde{\mathbf{t}}}\mathbf{H}_{\mathrm{LI}}^H\right\} \\ &= \mathcal{E}\left\{\left\|\Delta\tilde{\mathbf{H}}_{\mathrm{LI}}\hat{\mathbf{t}} + \mathbf{H}_{\mathrm{LI}}\Delta\tilde{\mathbf{t}}\right\|_2^2\right\}. \quad (13)\end{aligned}$$

If cancellation is not used, i.e., $\mathbf{C} = \mathbf{0}$, (12) reduces to (8).

The main drawback of TDC is its blindness to the spatial domain, e.g., low rank of $\mathbf{H}_{\mathrm{LI}}$ is not expected to result in better isolation. Additionally, the scheme is sensitive to both channel estimation noise $\Delta\tilde{\mathbf{H}}_{\mathrm{LI}}$ and transmit signal noise $\Delta\tilde{\mathbf{t}}$ as shown by (13). In fact, TDC adds a new signal in the relay input which may actually lead to degraded isolation compared to pure natural isolation with high channel estimation noise. The advantage of time-domain cancellation is that it does not distort the desired signal or reduce the input and output dimensions of the relay, i.e., $\hat{N}_{\mathrm{rx}} = N_{\mathrm{rx}}$ and $\hat{N}_{\mathrm{tx}} = N_{\mathrm{tx}}$.

B. Novel Spatial Suppression Schemes

To exploit the extra degrees of freedom offered by the spatial domain, we propose that the relay applies MIMO receive filter $\mathbf{G}_{\mathrm{rx}} \in \mathbb{C}^{\hat{N}_{\mathrm{rx}}\times N_{\mathrm{rx}}}$ and MIMO transmit filter $\mathbf{G}_{\mathrm{tx}} \in \mathbb{C}^{N_{\mathrm{tx}}\times\hat{N}_{\mathrm{tx}}}$ as illustrated in Fig. 3. Now (2), (5), and (7) can be related as $\hat{\mathbf{r}} = \mathbf{G}_{\mathrm{rx}}\mathbf{r}$, $\tilde{\mathbf{t}} = \mathbf{G}_{\mathrm{tx}}\hat{\mathbf{t}}$, $\mathbf{R}_{\tilde{\mathbf{t}}} = \mathbf{G}_{\mathrm{tx}}\mathbf{R}_{\hat{\mathbf{t}}}\mathbf{G}_{\mathrm{tx}}^H$, $\hat{\mathbf{H}}_{\mathrm{SR}} = \mathbf{G}_{\mathrm{rx}}\mathbf{H}_{\mathrm{SR}}$, and $\hat{\mathbf{H}}_{\mathrm{RD}} = \mathbf{H}_{\mathrm{RD}}\mathbf{G}_{\mathrm{tx}}$. Throughout the paper, we normalize filter gains to $\|\mathbf{G}_{\mathrm{rx}}\|_F^2 = N_{\mathrm{rx}}$ and $\|\mathbf{G}_{\mathrm{tx}}\|_F^2 = N_{\mathrm{tx}}$ with all schemes.

The equivalent receiver noise vector of the "interference-free" relay becomes

$$\hat{\mathbf{n}}_{\mathrm{R}} = \hat{\mathbf{H}}_{\mathrm{LI}}\hat{\mathbf{t}} + \mathbf{G}_{\mathrm{rx}}\mathbf{H}_{\mathrm{LI}}\Delta\tilde{\mathbf{t}} + \mathbf{G}_{\mathrm{rx}}\mathbf{n}_{\mathrm{R}} \quad (14)$$

in which the residual loop interference channel is

$$\hat{\mathbf{H}}_{\mathrm{LI}} = \mathbf{G}_{\mathrm{rx}}\mathbf{H}_{\mathrm{LI}}\mathbf{G}_{\mathrm{tx}} = \mathbf{G}_{\mathrm{rx}}\tilde{\mathbf{H}}_{\mathrm{LI}}\mathbf{G}_{\mathrm{tx}} + \mathbf{G}_{\mathrm{rx}}\Delta\tilde{\mathbf{H}}_{\mathrm{LI}}\mathbf{G}_{\mathrm{tx}}. \quad (15)$$

Based on (14), the residual interference power is given by

$$\begin{aligned}P_{\mathrm{I}} &= \mathcal{E}\left\{\left\|\hat{\mathbf{H}}_{\mathrm{LI}}\hat{\mathbf{t}} + \mathbf{G}_{\mathrm{rx}}\mathbf{H}_{\mathrm{LI}}\Delta\tilde{\mathbf{t}}\right\|_2^2\right\} \\ &= \mathrm{tr}\left\{\hat{\mathbf{H}}_{\mathrm{LI}}\mathbf{R}_{\hat{\mathbf{t}}}\hat{\mathbf{H}}_{\mathrm{LI}}^H\right\} + \mathrm{tr}\left\{\mathbf{G}_{\mathrm{rx}}\mathbf{H}_{\mathrm{LI}}\mathbf{R}_{\Delta\tilde{\mathbf{t}}}\mathbf{H}_{\mathrm{LI}}^H\mathbf{G}_{\mathrm{rx}}^H\right\}. \quad (16)\end{aligned}$$

Interference can be suppressed by designing $\mathbf{G}_{\mathrm{rx}}$ and $\mathbf{G}_{\mathrm{tx}}$ to minimize the first term and/or by designing only $\mathbf{G}_{\mathrm{rx}}$ to minimize the second term that is due to transmit signal noise. Since (15) is a matrix equation, it needs to be first translated into a scalar value before formulating an optimization problem: In this paper, the Frobenius norm is adopted for this purpose while other metrics, rendering different optimization targets, are also available. On the other hand, (16) for spatial suppression is reduced to mere natural isolation given in (9) when $\mathbf{G}_{\mathrm{rx}} = \mathbf{I}$ and $\mathbf{G}_{\mathrm{tx}} = \mathbf{I}$.

Spatial suppression comes at the cost of a reduction in the input or output dimensions comparing to TDC. However, (14) reveals readily one significant advantage over cancellation: the receive filter $\mathbf{G}_{\mathrm{rx}}$ can be designed to suppress the potential loop interference that is due to the transmit signal noise $\Delta\tilde{\mathbf{t}}$.

The implementation differs depending on the procedure:

- *Independent design*: One filter is designed without knowledge of the other filter which can be replaced by $\mathbf{I}$.
- *Separate design*: One filter is designed given the other.
- *Joint design*: The filters are designed together.

Next we consider these procedures with antenna selection, beam selection, null-space projection, and MMSE filtering.

1) Antenna Selection (AS): The simplified receive antenna selection scheme studied in [25] inspires us to formulate loop interference suppression based on generalized antenna subset selection. To that end, the respective receive and transmit filters are implemented with row and column selection matrices (see Section I-C) that are scaled to normalize the gains:

$$\mathbf{G}_{\mathrm{rx}} = \sqrt{\frac{N_{\mathrm{rx}}}{\hat{N}_{\mathrm{rx}}}}\mathbf{S}_{\mathrm{rx}}^T \text{ and } \mathbf{G}_{\mathrm{tx}} = \sqrt{\frac{N_{\mathrm{tx}}}{\hat{N}_{\mathrm{tx}}}}\mathbf{S}_{\mathrm{tx}}. \quad (17)$$

To reduce the gain of the residual loop interference channel given in (15), we define the objective for suppression as

$$\mathcal{J} = \min\|\mathbf{G}_{\mathrm{rx}}\tilde{\mathbf{H}}_{\mathrm{LI}}\mathbf{G}_{\mathrm{tx}}\|_F^2 \quad (18)$$

decreasing the known part of $\|\hat{\mathbf{H}}_{\mathrm{LI}}\|_F^2$. By substituting (17)

$$\mathcal{J}_{\mathrm{AS}} = \frac{N_{\mathrm{rx}}N_{\mathrm{tx}}}{\hat{N}_{\mathrm{rx}}\hat{N}_{\mathrm{tx}}}\min\|\mathbf{S}_{\mathrm{rx}}^T\tilde{\mathbf{H}}_{\mathrm{LI}}\mathbf{S}_{\mathrm{tx}}\|_F^2. \quad (19)$$

The optimal joint filter design is found by calculating the Frobenius norm for all $\binom{N_{\mathrm{rx}}}{\hat{N}_{\mathrm{rx}}}\binom{N_{\mathrm{tx}}}{\hat{N}_{\mathrm{tx}}}$ combinations and choosing the lowest. Although one may easily devise suboptimal methods of lower complexity, only global search gives the exact optimum in the general case. However, it is feasible because the number of antennas is in practice reasonably small.

Let us then consider the design of $\mathbf{S}_{\mathrm{rx}}^T$ to illustrate the separate filter design (the procedure is symmetric for designing $\mathbf{S}_{\mathrm{tx}}$). Now $\mathbf{G}_{\mathrm{tx}}$ needs to be first fixed based on any spatial suppression scheme and the unique solution for $\min\|\mathbf{S}_{\mathrm{rx}}^T\tilde{\mathbf{H}}_{\mathrm{LI}}\mathbf{G}_{\mathrm{tx}}\|_F^2$ is simply one of the $\binom{N_{\mathrm{rx}}}{\hat{N}_{\mathrm{rx}}}$ combinations. If the transmit filter is

TABLE I
ALGORITHM FOR OPTIMAL JOINT BEAM SELECTION

Design $\mathbf{S}_{\mathrm{rx}}^T$ and $\mathbf{S}_{\mathrm{tx}}$ to select $\hat{N}_{\mathrm{rx}}$ rows and $\hat{N}_{\mathrm{tx}}$ columns of $\tilde{\mathbf{\Sigma}}$ as follows.
Step 1: Select in total $\min\{\hat{N}_{\mathrm{rx}}+\hat{N}_{\mathrm{tx}}, \max\{N_{\mathrm{rx}}, N_{\mathrm{tx}}\}\}$ rows and columns such that all combinations pick only off-diagonal elements of $\tilde{\mathbf{\Sigma}}$. For this subsolution $\mathcal{J}_{\mathrm{BS}} = 0$.
Step 2: To satisfy objective $\mathcal{J}_{\mathrm{BS}}$, select the rest of the rows and columns such that the final selection matrices pick only the $\hat{N}_{\mathrm{rx}} + \hat{N}_{\mathrm{tx}} - \max\{N_{\mathrm{rx}}, N_{\mathrm{tx}}\}$ smallest singular values.

not known (as in independent filter design) or not yet selected, one can substitute $\mathbf{G}_{\mathrm{tx}} = \mathbf{I}$, which reduces the objective to $\min \|\mathbf{S}_{\mathrm{rx}}^T \tilde{\mathbf{H}}_{\mathrm{LI}}\|_F^2$.

Example 1: The scheme of [25] is limited to the special case of $N_{\mathrm{rx}} = 2$ and $\hat{N}_{\mathrm{rx}} = N_{\mathrm{tx}} = \hat{N}_{\mathrm{tx}} = 1$, i.e., $\mathbf{G}_{\mathrm{tx}} = 1$: When $\tilde{\mathbf{H}}_{\mathrm{LI}} = [\tilde{h}_1\ \tilde{h}_2]^T$, $\|\mathbf{S}_{\mathrm{rx}}^T \tilde{\mathbf{H}}_{\mathrm{LI}}\|_F^2$ is minimized by selecting $\mathbf{S}_{\mathrm{rx}}^T = [1\ 0]$ if $|\tilde{h}_1|^2 < |\tilde{h}_2|^2$ and $\mathbf{S}_{\mathrm{rx}}^T = [0\ 1]$ otherwise. In the general MIMO case of any N_{rx}, N_{tx}, $\hat{N}_{\mathrm{rx}}$, and $\hat{N}_{\mathrm{tx}}$, such single comparison is not sufficient for the optimal filter design that is solved in the above paragraphs for different variations.

2) Beam Selection (BS): General (eigen)beam selection is based on the singular value decomposition (SVD) of $\tilde{\mathbf{H}}_{\mathrm{LI}}$

$$\tilde{\mathbf{H}}_{\mathrm{LI}} = \tilde{\mathbf{U}}\tilde{\mathbf{\Sigma}}\tilde{\mathbf{V}}^H = [\tilde{\mathbf{U}}_{(1)}\ \tilde{\mathbf{U}}_{(0)}]\tilde{\mathbf{\Sigma}}[\tilde{\mathbf{V}}_{(1)}\ \tilde{\mathbf{V}}_{(0)}]^H \tag{20}$$

in which submatrices $\tilde{\mathbf{U}}_{(0)}$ and $\tilde{\mathbf{V}}_{(0)}$ contain the basis vectors associated with zero singular values. The diagonal matrix $\tilde{\mathbf{\Sigma}} \in \mathbb{R}^{N_{\mathrm{rx}} \times N_{\mathrm{tx}}}$ comprises the singular values $\tilde{\sigma}_n = \{\tilde{\mathbf{\Sigma}}\}_{n,n}$, $n = 1, 2, \ldots, \min\{N_{\mathrm{rx}}, N_{\mathrm{tx}}\}$, sorted in descending order.

By choosing beam selection matrices as

$$\mathbf{G}_{\mathrm{rx}} = \sqrt{\frac{N_{\mathrm{rx}}}{\hat{N}_{\mathrm{rx}}}}\mathbf{S}_{\mathrm{rx}}^T \tilde{\mathbf{U}}^H \text{ and } \mathbf{G}_{\mathrm{tx}} = \sqrt{\frac{N_{\mathrm{tx}}}{\hat{N}_{\mathrm{tx}}}}\tilde{\mathbf{V}}\mathbf{S}_{\mathrm{tx}} \tag{21}$$

the objective is transformed from (18) to

$$\mathcal{J}_{\mathrm{BS}} = \frac{N_{\mathrm{rx}}N_{\mathrm{tx}}}{\hat{N}_{\mathrm{rx}}\hat{N}_{\mathrm{tx}}} \min \|\mathbf{S}_{\mathrm{rx}}^T \tilde{\mathbf{\Sigma}} \mathbf{S}_{\mathrm{tx}}\|_F^2 \tag{22}$$

as $\tilde{\mathbf{U}}^H\tilde{\mathbf{U}} = \mathbf{I}$, $\tilde{\mathbf{V}}^H\tilde{\mathbf{V}} = \mathbf{I}$ by definition. Filter design becomes conceptually similar to AS, but row and column selection is based on the effective diagonal channel $\tilde{\mathbf{\Sigma}}$ instead of $\tilde{\mathbf{H}}_{\mathrm{LI}}$.

Remark 3: Objective $\mathcal{J}_{\mathrm{BS}}$ readily indicates that BS is superior to AS. In (22) most row and column combinations pick off-diagonal elements of $\tilde{\mathbf{\Sigma}}$ that are zero by definition leading to $\mathcal{J}_{\mathrm{BS}} = 0$ for many subsolutions whereas in (19) all elements of $\tilde{\mathbf{H}}_{\mathrm{LI}}$ are practically nonzero, i.e., $\mathcal{J}_{\mathrm{AS}} > 0$ for all subsolutions. In other words, AS is optimal only when limiting the search space to binary selection matrices while BS solves the optimization target with general complex matrices.

Intuitively, the optimal joint BS could be solved by testing all $\binom{N_{\mathrm{rx}}}{\hat{N}_{\mathrm{rx}}}\binom{N_{\mathrm{tx}}}{\hat{N}_{\mathrm{tx}}}$ combinations as with AS. However, the diagonalized structure of the effective loop channel facilitates direct offline selection based on N_{rx}, N_{tx}, $\hat{N}_{\mathrm{rx}}$, and $\hat{N}_{\mathrm{tx}}$ such that only the SVD is calculated for each channel representation: The optimal joint selection is obtained with the algorithm given in Table I. If $\hat{N}_{\mathrm{rx}} + \hat{N}_{\mathrm{tx}} \leq \max\{N_{\mathrm{rx}}, N_{\mathrm{tx}}\}$, *Step 2* is omitted and BS reduces to null-space projection discussed in the next section. On the other hand, separate and independent filter designs apply only *Step 2* for all $\hat{N}_{\mathrm{rx}} + \hat{N}_{\mathrm{tx}}$ rows and columns.

Let us assume that $\hat{N}_{\mathrm{rx}} + \hat{N}_{\mathrm{tx}} > \max\{N_{\mathrm{rx}}, N_{\mathrm{tx}}\}$ in the following. One straightforward illustrative solution can be obtained with the optimal joint BS algorithm as

$$\mathbf{S}_{\mathrm{rx}}^T \tilde{\mathbf{\Sigma}} \mathbf{S}_{\mathrm{tx}} = \begin{bmatrix} \mathbf{I}_{\mathrm{rx1}} & \mathbf{0} & \mathbf{0} \\ \mathbf{0} & \mathbf{0} & \mathbf{I}_{\mathrm{rx2}} \end{bmatrix} \tilde{\mathbf{\Sigma}} \begin{bmatrix} \mathbf{0} \\ \mathbf{I}_{\mathrm{tx}} \end{bmatrix} \tag{23}$$

in which $\mathbf{I}_{\mathrm{rx1}}$, $\mathbf{I}_{\mathrm{rx2}}$ and $\mathbf{I}_{\mathrm{tx}}$ are identity matrices of $(N_{\mathrm{tx}} - \hat{N}_{\mathrm{tx}})$, $(\hat{N}_{\mathrm{rx}} + \hat{N}_{\mathrm{tx}} - N_{\mathrm{tx}})$ and $\hat{N}_{\mathrm{tx}}$ dimensions, respectively. In fact, the optimal joint BS algorithm translates (22) to

$$\mathcal{J}_{\mathrm{BS}} = \frac{N_{\mathrm{rx}}N_{\mathrm{tx}}}{\hat{N}_{\mathrm{rx}}\hat{N}_{\mathrm{tx}}} \sum_{n=N_{\mathrm{rx}}-\hat{N}_{\mathrm{rx}}+N_{\mathrm{tx}}-\hat{N}_{\mathrm{tx}}+1}^{\min\{N_{\mathrm{rx}},N_{\mathrm{tx}}\}} \tilde{\sigma}_n^2. \tag{24}$$

For the general case, this shows that BS may cause residual loop interference even if the side information is perfect. In the next section, this motivates to consider the special cases of beam selection that ideally eliminate all interference.

Example 2: Compared to our general BS solution, the scheme of [28] is not only suboptimal but also limited to the special symmetric case of $N_{\mathrm{rx}} = N_{\mathrm{tx}}$ and $\hat{N}_{\mathrm{rx}} = \hat{N}_{\mathrm{tx}}$: The beams are selected by $\mathbf{S}_{\mathrm{rx}} = \mathbf{S}_{\mathrm{tx}} = [\mathbf{0}\,|\,\mathbf{I}]^T$ in which $\mathbf{0}$ is an $\hat{N}_{\mathrm{rx}} \times (N_{\mathrm{rx}} - \hat{N}_{\mathrm{rx}})$ zero matrix and $\mathbf{I}$ is an $\hat{N}_{\mathrm{rx}} \times \hat{N}_{\mathrm{rx}}$ identity matrix. This picks the $\hat{N}_{\mathrm{rx}}$ smallest singular values transforming (22) to

$$\mathcal{J}_{[28]} = \frac{N_{\mathrm{rx}}^2}{\hat{N}_{\mathrm{rx}}^2} \sum_{n=N_{\mathrm{rx}}-\hat{N}_{\mathrm{rx}}+1}^{N_{\mathrm{rx}}} \tilde{\sigma}_n^2 > \mathcal{J}_{\mathrm{BS}}. \tag{25}$$

This is larger than (24) obtained with (23) because the scheme does not exploit the possibility to suppress interference by picking the off-diagonal elements of $\tilde{\mathbf{\Sigma}}$ in *Step 1*. The suboptimality can be also interpreted to be the consequence of independent filter design instead of joint design.

3) Null-Space Projection (NSP): Next we develop spatial suppression schemes that can eliminate all loop interference in the ideal case with perfect side information similarly to TDC. This is desirable when the loop interference is dominating but AS or general BS does not offer sufficient attenuation.

In null-space projection, $\mathbf{G}_{\mathrm{rx}}$ and $\mathbf{G}_{\mathrm{tx}}$ are selected such that the relay receives and transmits in different subspaces, i.e., transmit beams are projected to the null-space of the loop channel combined with the receive filter and vice versa. The condition can be stated for joint or separate filter design as

$$\mathbf{G}_{\mathrm{rx}} \tilde{\mathbf{H}}_{\mathrm{LI}} \mathbf{G}_{\mathrm{tx}} = \mathbf{0} \tag{26}$$

to eliminate the known part of the first term in (16). Similarly, for suppressing the transmit signal noise, the condition becomes $\mathbf{G}_{\mathrm{rx}} \tilde{\mathbf{H}}_{\mathrm{LI}} = \mathbf{0}$, partly eliminating the second term in (16).

One solution for joint NSP can be obtained with the optimal joint BS algorithm given in Table I, if $\hat{N}_{\mathrm{rx}}$, $\hat{N}_{\mathrm{tx}}$ and $\mathrm{rk}\{\tilde{\mathbf{H}}_{\mathrm{LI}}\}$ are low enough w.r.t. N_{rx} and N_{tx}. Firstly, a total of $\max\{N_{\mathrm{rx}}, N_{\mathrm{tx}}\}$ beams are selected in *Step 1* corresponding to different singular values. Secondly, the last terms in (24) are zero if $\mathrm{rk}\{\tilde{\mathbf{H}}_{\mathrm{LI}}\} < \min\{N_{\mathrm{rx}}, N_{\mathrm{tx}}\}$. Thus, $\min\{N_{\mathrm{rx}}, N_{\mathrm{tx}}\} - \mathrm{rk}\{\tilde{\mathbf{H}}_{\mathrm{LI}}\}$ input and output beams may correspond to the same singular values after *Step 2* and still $\mathcal{J}_{\mathrm{BS}} = 0$, i.e., $\mathbf{S}_{\mathrm{rx}}^T \tilde{\mathbf{\Sigma}} \mathbf{S}_{\mathrm{tx}} = \mathbf{0}$ satisfying also the condition in

(26). This proves that the BS algorithm results in null-space projection whenever

$$\hat{N}_{\rm rx} + \hat{N}_{\rm tx} + {\rm rk}\left\{\tilde{\mathbf{H}}_{\rm LI}\right\} \leq N_{\rm rx} + N_{\rm tx}. \tag{27}$$

This condition defines also the general existence of joint NSP, if $\mathbf{G}_{\rm rx}$ and $\mathbf{G}_{\rm tx}$ are additionally constrained to be of full rank.

Even if $\mathbf{H}_{\rm LI}$ is rank deficient, $\tilde{\mathbf{H}}_{\rm LI}$ is of full rank in practice due to the estimation noise which also causes residual loop interference. Thereby, the condition in (27) can be alternatively evaluated using the anticipated value of ${\rm rk}\,\{\mathbf{H}_{\rm LI}\}$ based on prior information or by defining ${\rm rk}\{\tilde{\mathbf{H}}_{\rm LI}\}$ with a threshold below which the singular values are rounded to zero.

Remark 4: For the case $\hat{N}_{\rm rx} = \hat{N}_{\rm tx}$, the total number for antennas $(N_{\rm rx} + N_{\rm tx})$ is minimized with NSP by selecting $N_{\rm rx} = 2\hat{N}_{\rm rx} = 2N_{\rm tx} = 2\hat{N}_{\rm tx}$ or $N_{\rm tx} = 2\hat{N}_{\rm tx} = 2N_{\rm rx} = 2\hat{N}_{\rm rx}$ when ${\rm rk}\{\tilde{\mathbf{H}}_{\rm LI}\} = \min\{N_{\rm rx}, N_{\rm tx}\}$ (full rank), or by selecting $N_{\rm rx} = \hat{N}_{\rm rx} + 1 = N_{\rm tx} + 1 = \hat{N}_{\rm tx} + 1$ or $N_{\rm tx} = \hat{N}_{\rm tx} + 1 = N_{\rm rx} + 1 = \hat{N}_{\rm rx} + 1$ when ${\rm rk}\{\tilde{\mathbf{H}}_{\rm LI}\} = 1$ (minimum rank). Choosing $N_{\rm rx} > N_{\rm tx}$ may be preferable due to transmit noise.

For separate filter design, let us recall that the Moore-Penrose pseudoinverse $\mathbf{X}^+$ is unique, always exists, and satisfies $\mathbf{X}\mathbf{X}^+\mathbf{X} = \mathbf{X}$ by definition. For designing $\mathbf{G}_{\rm rx}$ separately given $\mathbf{G}_{\rm tx}$, we can, thereby, apply projection matrix

$$\mathbf{G}_{\rm rx} = \sqrt{\frac{N_{\rm rx}}{N_{\rm rx} - {\rm rk}\{\tilde{\mathbf{H}}_{\rm LI}\mathbf{G}_{\rm tx}\}}}\left(\mathbf{I} - \tilde{\mathbf{H}}_{\rm LI}\mathbf{G}_{\rm tx}\left(\tilde{\mathbf{H}}_{\rm LI}\mathbf{G}_{\rm tx}\right)^+\right) \tag{28}$$

if ${\rm rk}\{\tilde{\mathbf{H}}_{\rm LI}\mathbf{G}_{\rm tx}\} < N_{\rm rx}$. Separate design for $\mathbf{G}_{\rm tx}$ is given by a similar projection matrix which is obtained by replacing $\tilde{\mathbf{H}}_{\rm LI}\mathbf{G}_{\rm tx}$ and $N_{\rm rx}$ above with $\mathbf{G}_{\rm rx}\tilde{\mathbf{H}}_{\rm LI}$ and $N_{\rm tx}$, respectively.

Example 3: The scheme of [27] is limited to the simple special case of $N_{\rm rx} = \hat{N}_{\rm rx} = \hat{N}_{\rm tx} = 1$ and $N_{\rm tx} = 2$: When $\tilde{\mathbf{H}}_{\rm LI} = [\tilde{h}_1\ \tilde{h}_2]$, $\tilde{\mathbf{H}}_{\rm LI}\mathbf{G}_{\rm tx} = 0$ is guaranteed directly by $\mathbf{G}_{\rm tx} = \frac{\sqrt{2}[\pm\tilde{h}_2 \mp\tilde{h}_1]^T}{\sqrt{|\tilde{h}_1|^2+|\tilde{h}_2|^2}}$. In the general MIMO case of any $N_{\rm rx}$, $N_{\rm tx}$, $\hat{N}_{\rm rx}$, and $\hat{N}_{\rm tx}$, the optimal filter design, solved in the above paragraphs, becomes more involved.

For designing one filter independently, the above schemes may be exploited by setting the other filter to identity. However, simpler design is obtained by choosing $\mathbf{G}_{\rm rx} = \sqrt{\frac{N_{\rm rx}}{(N_{\rm rx} - {\rm rk}\{\tilde{\mathbf{H}}_{\rm LI}\})}}\tilde{\mathbf{U}}_{(0)}^H$ because the row space of $\mathbf{G}_{\rm rx}$ should be in the left null space of $\tilde{\mathbf{H}}_{\rm LI}$ or by choosing $\mathbf{G}_{\rm tx} = \sqrt{\frac{N_{\rm tx}}{(N_{\rm tx} - {\rm rk}\{\tilde{\mathbf{H}}_{\rm LI}\})}}\tilde{\mathbf{V}}_{(0)}$ because the column space of $\mathbf{G}_{\rm tx}$ should be in the null space of $\tilde{\mathbf{H}}_{\rm LI}$.

Joint design solutions satisfying the NSP condition in (26) are not unique in most cases. For example, *Step 1* in the optimal joint BS algorithm allows to choose rows and columns in different ways. Furthermore, general BS inherits the same property except that the subsolution picking the nonzero diagonal values of $\tilde{\mathbf{\Sigma}}$ is unique in *Step 2*. Selection between the solutions with the same cost can be done based on any other performance criterion as illustrated by the next example.

Example 4: The scheme of [26] is limited to the case of $N_{\rm rx} = N_{\rm tx} = 2$ and $\hat{N}_{\rm rx} = \hat{N}_{\rm tx} = 1$: When the SVD of the loop channel is $\tilde{\mathbf{H}}_{\rm LI} = [\tilde{\mathbf{u}}_1\ \tilde{\mathbf{u}}_2]\tilde{\mathbf{\Sigma}}[\tilde{\mathbf{v}}_1\ \tilde{\mathbf{v}}_2]^H$, $\mathbf{G}_{\rm rx}\tilde{\mathbf{H}}_{\rm LI}\mathbf{G}_{\rm tx} = 0$ is guaranteed either by $\mathbf{G}_{\rm rx} = \sqrt{2}\tilde{\mathbf{u}}_1^H$, $\mathbf{G}_{\rm tx} = \sqrt{2}\tilde{\mathbf{v}}_2$ or by $\mathbf{G}_{\rm rx} = \sqrt{2}\tilde{\mathbf{u}}_2^H$, $\mathbf{G}_{\rm tx} = \sqrt{2}\tilde{\mathbf{v}}_1$. Although not recognized in [26], also $\mathbf{G}_{\rm rx} = \sqrt{2}\tilde{\mathbf{u}}_2^H$, $\mathbf{G}_{\rm tx} = \sqrt{2}\tilde{\mathbf{v}}_2$ can be used if ${\rm rk}\{\tilde{\mathbf{H}}_{\rm LI}\} = 1$. Compared to Example 3, the extra receive antenna facilitates additional selection diversity available for reducing the effect of transmit signal noise. In our general MIMO case of any $N_{\rm rx}$, $N_{\rm tx}$, $\hat{N}_{\rm rx}$, and $\hat{N}_{\rm tx}$, the optimal filter design becomes more involved and the applicability of NSP is governed by (27).

4) Minimum Mean Square Error (MMSE) Filtering: The previous spatial suppression schemes aim at minimizing the effect of loop interference at the cost of spatially shaping the useful signal which does not happen with TDC. In order to reduce the effect of this drawback with spatial suppression, a minimum MSE scheme is developed next to both minimize the distortion and attenuate the loop interference.

Now $\hat{N}_{\rm rx} = N_{\rm rx}$ and $\hat{N}_{\rm tx} = N_{\rm tx}$ as with TDC. Thus, the MSE matrix of the relay input signal is given by

$$\begin{aligned}\mathbf{M} &= \mathcal{E}\left\{\left(\mathbf{H}_{\rm SR}\mathbf{x} - \hat{\mathbf{r}}\right)\left(\mathbf{H}_{\rm SR}\mathbf{x} - \hat{\mathbf{r}}\right)^H\right\} \\ &= \left(\mathbf{I} - \mathbf{G}_{\rm rx}\right)\mathbf{H}_{\rm SR}\mathbf{R}_{\mathbf{x}}\mathbf{H}_{\rm SR}^H\left(\mathbf{I} - \mathbf{G}_{\rm rx}^H\right) + \mathbf{R}_{\hat{\mathbf{n}}_{\rm R}}\end{aligned} \tag{29}$$

in which $\mathbf{R}_{\hat{\mathbf{n}}_{\rm R}} = \mathcal{E}\{\hat{\mathbf{n}}_{\rm R}\hat{\mathbf{n}}_{\rm R}^H\} = \mathbf{G}_{\rm rx}(\mathbf{H}_{\rm LI}\mathbf{R}_{\mathbf{t}}\mathbf{H}_{\rm LI}^H + \mathbf{R}_{\mathbf{n}_{\rm R}})\mathbf{G}_{\rm rx}^H$. For separate filter design given $\mathbf{G}_{\rm tx}$, the minimum MSE receive filter is derived from the condition $\frac{\partial}{\partial \mathbf{G}_{\rm rx}}{\rm tr}\{\mathbf{M}\} = \mathbf{0}$ yielding

$$\mathbf{G}_{\rm rx} = \tilde{\mathbf{H}}_{\rm SR}\mathbf{R}_{\mathbf{x}}\tilde{\mathbf{H}}_{\rm SR}^H\left(\tilde{\mathbf{H}}_{\rm SR}\mathbf{R}_{\mathbf{x}}\tilde{\mathbf{H}}_{\rm SR}^H + \tilde{\mathbf{H}}_{\rm LI}\mathbf{R}_{\mathbf{t}}\tilde{\mathbf{H}}_{\rm LI}^H + \mathbf{R}_{\mathbf{n}_{\rm R}}\right)^{-1} \tag{30}$$

which needs to be scaled to satisfy $\|\mathbf{G}_{\rm rx}\|_F^2 = N_{\rm rx}$. Note that MMSE filtering requires knowledge of $\mathbf{H}_{\rm SR}$ and signal covariance matrices as opposed to the other mitigation schemes.

Condition $\frac{\partial}{\partial \mathbf{G}_{\rm tx}}{\rm tr}\{\mathbf{M}\} = \mathbf{0}$ to minimize MSE at the transmit side reduces to the condition for null-space projection given in (26). Therefore, the evident order for joint filter design is to firstly minimize interference at the transmit side using any scheme, and then secondly design the receive filter using (30).

5) Combining Cancellation and Spatial Suppression: Time-domain cancellation suffers from residual interference that is due to the transmit signal noise, while spatial suppression may need many extra antennas for efficient mitigation. Hence, the combination could offer high isolation with conservative number of antennas in the presence of transmit signal noise.

Combining yields the residual interference channel given by $\hat{\mathbf{H}}_{\rm LI} = \mathbf{G}_{\rm rx}\mathbf{H}_{\rm LI}\mathbf{G}_{\rm tx} + \mathbf{C}$, cf. (11) with mere cancellation and (15) with mere suppression. Thus, filter design can be performed for one scheme first if the other scheme is consequently designed given the residual channel. The implementation admits four variations for independent and separate filter design [32], but we will now focus on joint filter design, which is possible in most scenarios.

IV. Simulation Results

In this section, we evaluate and compare the performance of the mitigation schemes. In the simulations, all channels are modeled with Rayleigh fading and the transmitted signals are assumed to be spatially white with unit power per stream, thus $\mathbf{R}_{\mathbf{x}} = \mathbf{I}$ and $\mathbf{R}_{\hat{\mathbf{t}}} = \mathbf{I}$. The relay receiver noise is white and Gaussian with $\mathbf{R}_{\mathbf{n}_{\rm R}} = \mathbf{I}$, and imperfect side information used in mitigation is generated as explained in Section II-B.

Fig. 4 shows bit-error rate (BER) for a specific example setup with a decode-and-forward relay that uses linear zero-forcing

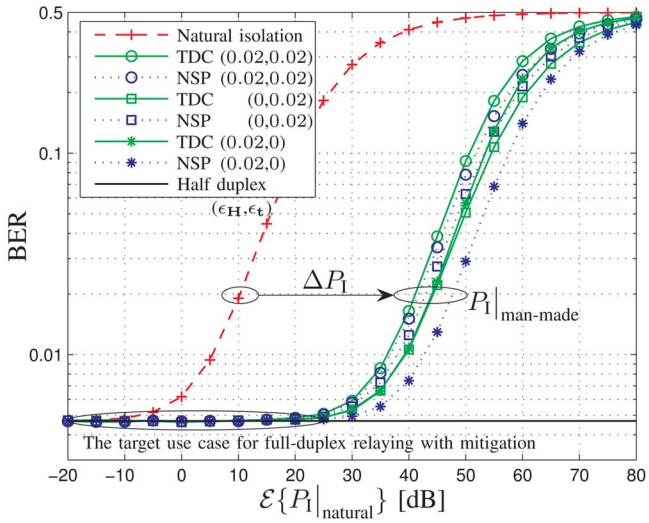

Fig. 4. BER of quadrature phase-shift keying at a decode-and-forward relay with zero-forcing when $N_{\mathrm{S}} = N_{\mathrm{rx}} = \hat{N}_{\mathrm{rx}} = \hat{N}_{\mathrm{tx}} = 3, \mathrm{rk}\{\mathbf{H}_{\mathrm{LI}}\} = 1$, and desired signal-to-noise ratio (SNR) is 25 dB. We choose $N_{\mathrm{tx}} = 3$ for natural isolation and TDC and $N_{\mathrm{tx}} = 4$ for beam selection that reduces to NSP in this setup.

detector for independent streams transmitted at different antennas. With proper self-interference mitigation or with large natural isolation, a full-duplex relay link achieves the same BER as its half-duplex counterpart, but offers significantly higher spectral efficiency by forwarding two symbols from the source to the destination within a time interval during which a half-duplex relay forwards only one. This explains also the target for interference mitigation and the use case for the full-duplex mode: It can be chosen over the half-duplex mode whenever the *residual* interference is weak enough such that it does not affect BER or similar performance metrics.

We see that interference mitigation manifests itself as a shift in the BER which is referred to as the *isolation improvement* obtained with signal processing w.r.t. natural isolation

$$\Delta P_{\mathrm{I}} = \frac{P_{\mathrm{I}}|_{\text{natural}}}{P_{\mathrm{I}}|_{\text{man-made}}} \tag{31}$$

for which $P_{\mathrm{I}}|_{\text{natural}}$ is given by (9), and $P_{\mathrm{I}}|_{\text{man-made}}$ is given by (13) with time-domain cancellation or (16) with spatial suppression. The observed shift is unique for each mitigation scheme, but essentially similar for all relaying protocols, system setups and performance metrics. Thus, we will evaluate the performance of the mitigation schemes by studying directly the statistics of ΔP_{I}: Its cumulative distribution function $F_{\Delta P_{\mathrm{I}}}(\cdot)$ and the average isolation improvement $\mathcal{E}\{\Delta P_{\mathrm{I}}\}$.

The isolation improvement is a versatile metric for evaluating the performance of mitigation and the intuitive choice because the schemes are formulated to minimize the self-interference power. Given any level of natural isolation, the statistics of ΔP_{I} show comprehensively how different schemes are affected by the errors of side information (parametrized with $\epsilon_{\mathbf{H}}$ and $\epsilon_{\mathbf{t}}$), configurations for antennas $(N_{\mathrm{rx}} \times N_{\mathrm{tx}})$ or streams $(\hat{N}_{\mathrm{rx}} \times \hat{N}_{\mathrm{tx}})$ and the loop channel rank $(\mathrm{rk}\{\mathbf{H}_{\mathrm{LI}}\})$.

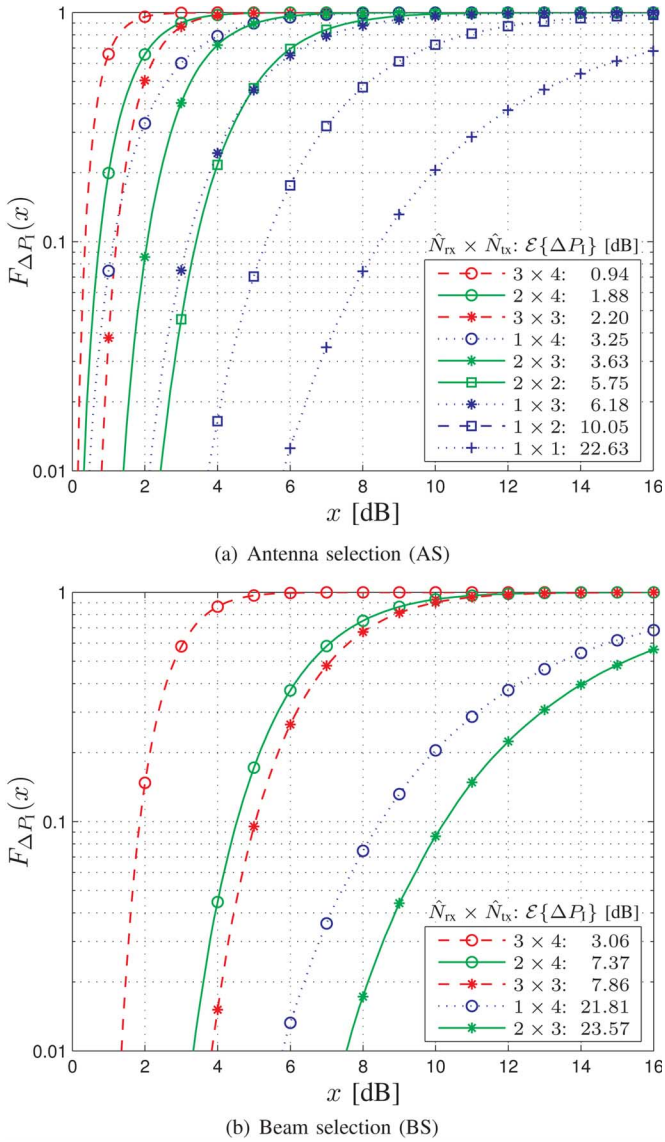

Fig. 5. The performance of the selection schemes when $N_{\mathrm{rx}} = N_{\mathrm{tx}} = 4$, the side information is perfect $(\epsilon_{\mathbf{H}} = \epsilon_{\mathbf{t}} = 0)$, and $\mathbf{H}_{\mathrm{LI}}$ is of full rank.

A. Performance With and Without Perfect Side Information

Let us first focus on schemes that are subject to residual interference even if the relay has perfect side information for mitigation $(\epsilon_{\mathbf{H}} = \epsilon_{\mathbf{t}} = 0)$. Fig. 5(a) and (b) illustrate the additional isolation brought by antenna and beam selection, respectively, when the loop channel is of full rank. The plots show the cumulative distribution functions for different input and output stream configurations $(\hat{N}_{\mathrm{rx}} \times \hat{N}_{\mathrm{tx}})$ and the legend tabulates the average isolation improvement. With the chosen parameters, BS reduces to NSP and all interference is blocked $(\Delta P_{\mathrm{I}} \to \infty)$ if $\hat{N}_{\mathrm{rx}} + \hat{N}_{\mathrm{tx}} \leq 4$. Fig. 6 illustrates how the rank of the interference channel affects the selection schemes with different receive and transmit antenna configurations $(N_{\mathrm{rx}} \times N_{\mathrm{tx}})$. The plots show the distributions and average values are tabulated in the legend. Now BS reduces to NSP, whenever $N_{\mathrm{rx}} + N_{\mathrm{tx}} \geq 6 + \mathrm{rk}\{\mathbf{H}_{\mathrm{LI}}\}$. Because AS offers low isolation w.r.t. the other schemes, it is omitted in later plots.

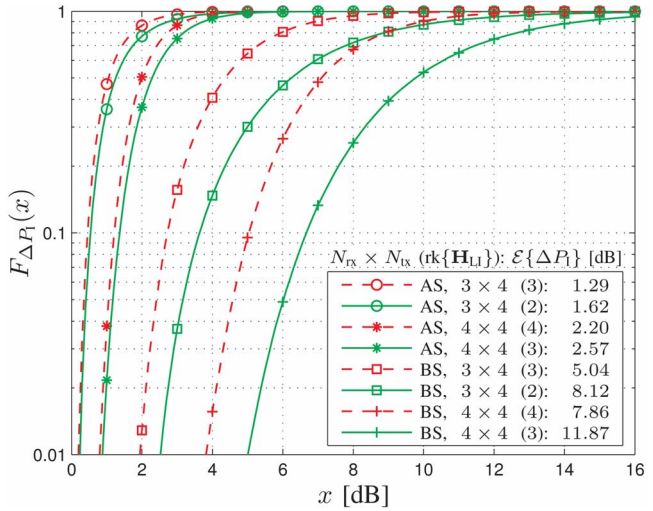

Fig. 6. The effect of loop channel rank on antenna and beam selection (AS and BS) when $\hat{N}_{\rm rx} = \hat{N}_{\rm tx} = 3$ and the side information is perfect ($\epsilon_{\mathbf{H}} = \epsilon_{\mathbf{t}} = 0$).

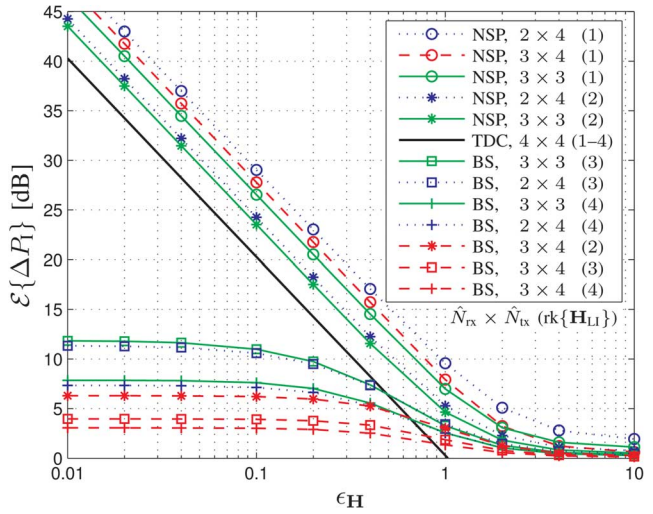

Fig. 7. The effect of channel estimation noise when $N_{\rm rx} = N_{\rm tx} = 4$ and $\epsilon_{\mathbf{t}} = 0$. BS reduces to NSP if $\hat{N}_{\rm rx} + \hat{N}_{\rm tx} + {\rm rk}\{\mathbf{H}_{\rm LI}\} \leq 8$.

Let us then continue to the practical case of using imperfect side information. Fig. 7 illustrates how the channel estimation noise, parametrized by $\epsilon_{\mathbf{H}}$, degrades the average isolation improvement. The side information on the transmitted signal is ideal in this plot. Thus, $\Delta P_{\rm I} \to \infty$ with time-domain cancellation and null-space projection when $\epsilon_{\mathbf{H}} \to 0$. Both time-domain cancellation and spatial suppression are sensitive to channel estimation noise. For low channel estimation noise, the average isolation improvement of TDC and NSP is linearly proportional to the relative estimation noise on a log-log scale with some constant gain which depends on the number of antennas, the rank of the loop channel, and the number of input and output streams. With perfect side information, the mitigation schemes always improve isolation. However, TDC may actually degrade the isolation with high estimation error because it adds new signal in the relay input contrary to spatial suppression that only filters the existing signals.

Fig. 8 illustrates how the transmit signal noise, parametrized by $\epsilon_{\mathbf{t}}$, degrades the average isolation improvement. The figure

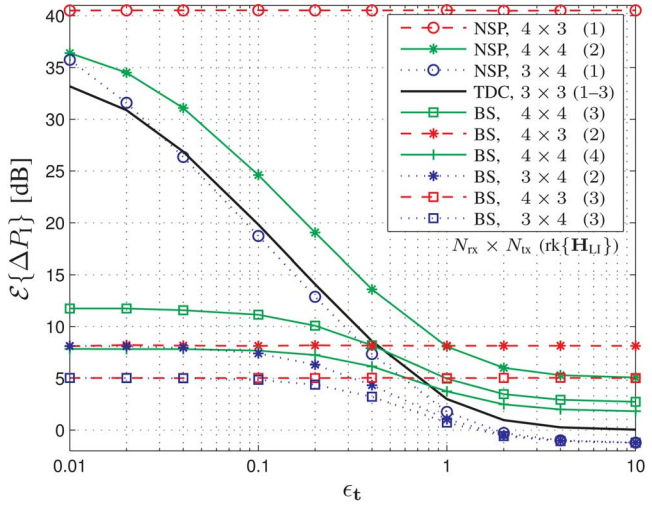

Fig. 8. The effect of transmit signal noise when $\hat{N}_{\rm rx} = \hat{N}_{\rm tx} = 3$ and $\epsilon_{\mathbf{H}} = 0.02$. BS reduces to NSP if $N_{\rm rx} + N_{\rm tx} - {\rm rk}\{\mathbf{H}_{\rm LI}\} \geq 6$.

also reveals the joint effect of the two imperfections in the side information. The selection diversity due to many equal BS and NSP solutions is exploited by choosing the solution that reduces the effect of the transmit signal noise the most. Consequently, BS and NSP become immune to the transmit signal noise whenever the degrees of freedom are sufficiently high at the relay receiver side.

B. MMSE and the Combination of TDC and Suppression

Fig. 9 compares MMSE suppression with the other schemes in terms of both the cumulative distribution function and the average isolation improvement. In this setup, MMSE and TDC have the same number of antennas which is sufficient to avoid the distortion of the useful signal. On the other hand, BS and NSP are implemented by adding an extra antenna at the receiver side which is needed in order to suppress interference at all. In general, the rank of the loop channel defines which scheme is preferable. The variance of the isolation improvement is considerably higher in spatial suppression than in TDC. The average isolation improvement of NSP and MMSE is approximately the same with rank-one loop channel, but MMSE yields larger variance.

Fig. 10 illustrates the benefit of combining time-domain cancellation and spatial suppression assuming joint filter design. The difference to separate or independent filter design is minimal because $N_{\rm rx}$ and $N_{\rm tx}$ are close to $\hat{N}_{\rm rx}$ and $\hat{N}_{\rm tx}$. We see that the combination of time-domain cancellation and spatial suppression offers better performance than either alone, except when the rank-deficient loop channel enables the usage of NSP. Then adding TDC to suppression may actually reduce the performance due to the transmit signal noise.

C. Discussion

In general, the simulation results show that spatial suppression is better than time-domain cancellation whenever there is a sufficient number of antennas compared to the number of spatial streams. However, the level of isolation is more stable in

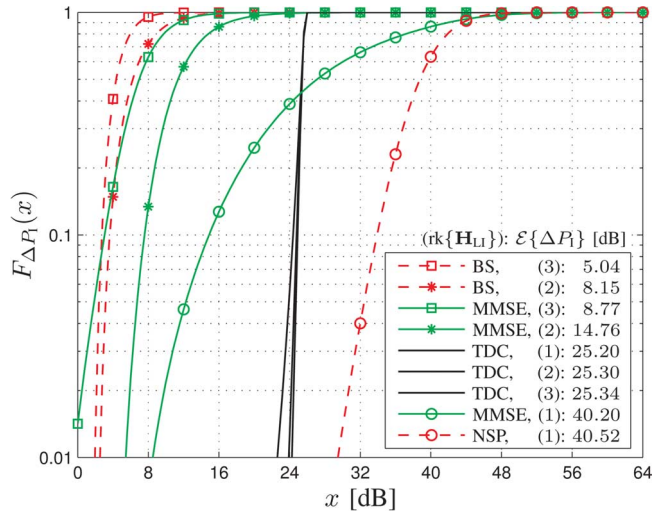

Fig. 9. Comparison of MMSE suppression and the other mitigation schemes when $N_{\mathrm{S}} = \hat{N}_{\mathrm{rx}} = N_{\mathrm{tx}} = \hat{N}_{\mathrm{tx}} = 3$, $\epsilon_{\mathbf{H}} = 0.02$, and $\epsilon_{\mathbf{t}} = 0.05$. We choose $N_{\mathrm{rx}} = 3$ for MMSE suppression and TDC and $N_{\mathrm{rx}} = 4$ for BS and NSP.

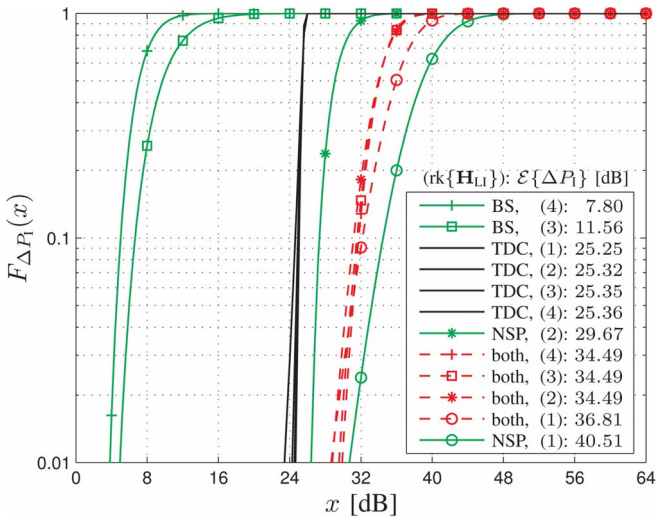

Fig. 10. The performance of the combination of TDC and spatial suppression when $\hat{N}_{\mathrm{rx}} = \hat{N}_{\mathrm{tx}} = 3$, $N_{\mathrm{rx}} = N_{\mathrm{tx}} = 4$, $\epsilon_{\mathbf{H}} = 0.02$, and $\epsilon_{\mathbf{t}} = 0.05$.

TDC than in spatial suppression which can be seen from the figures, e.g., by comparing the first percentile to the average. When it is beneficial to limit the distortion of the useful signal, TDC and MMSE filtering are preferred. The combination of TDC and spatial suppression is especially beneficial if there is significant amount of transmit signal noise.

The performance of spatial suppression depends highly on the rank of the loop channel. In fact, it can be postulated as a rule of thumb that spatial suppression is superior to cancellation whenever null-space projection is applicable. On the contrary, the rank has minimal effect on the performance of time-domain cancellation, e.g., isolation improvement is essentially the same irrespective of the rank in Figs. 7 and 8. Actually, lower rank leads to slightly worse performance due to the transmit noise in Figs. 9 and 10.

Without the transmit signal noise, the performance of all mitigation schemes is symmetric w.r.t. the number of antennas and streams. Thus, the performance stays the same if N_{rx} and $\hat{N}_{\mathrm{rx}}$ are swapped with N_{tx} and $\hat{N}_{\mathrm{tx}}$, respectively, in Figs. 5–7. The effect of the transmit signal noise breaks the symmetry and, in general, $N_{\mathrm{rx}} > N_{\mathrm{tx}}$ is better than $N_{\mathrm{rx}} < N_{\mathrm{tx}}$.

Antenna selection improves isolation modestly, and its performance is not comparable to the other schemes. In the example case of Fig. 5(a), only one transmit and receive antenna can be selected from the total of eight antennas to yield significant isolation improvement. However, AS could be adopted if it is sufficient to decrease the interference without complete elimination, e.g., if the natural isolation is already large and there are a couple of extra antennas to spare. In particular, AS needs less transceiver radio-frequency front-ends than antennas contrary to the other mitigation schemes.

V. Conclusion

Full-duplex MIMO relaying has large potential for spectrally efficient wireless transmission. In this paper, we concentrated on solving the main associated technical problem, i.e., the mitigation of relay self-interference. We extended the earlier SISO cancellation schemes for the MIMO relay case and proposed new solutions that suppress the interference in the spatial domain: antenna and beam selection, null-space projection, and MMSE filtering. We also discussed the issues that need to be considered when combining cancellation and spatial suppression. Errors in the side information used for mitigation were identified as the practical limitation to prevent complete interference elimination obtainable in the ideal case. However, our simulations illustrated that the proposed schemes offer significant mitigation such that the residual interference may be regarded as mere additional noise.

References

[1] C.-B. Chae, T. Tang, R. W. Heath, Jr, and S. Cho, "MIMO relaying with linear processing for multiuser transmission in fixed relay networks," *IEEE Trans. Signal Process.*, vol. 56, no. 2, pp. 727–738, Feb. 2008.

[2] R. Zhang, C. C. Chai, and Y.-C. Liang, "Joint beamforming and power control for multiantenna relay broadcast channel with QoS constraints," *IEEE Trans. Signal Process.*, vol. 57, no. 2, pp. 726–737, Feb. 2009.

[3] B. K. Chalise and L. Vandendorpe, "MIMO relay design for multipoint-to-multipoint communications with imperfect channel state information," *IEEE Trans. Signal Process.*, vol. 57, no. 7, pp. 2785–2796, Jul. 2009.

[4] Y. Rong, X. Tang, and Y. Hua, "A unified framework for optimizing linear nonregenerative multicarrier MIMO relay communication systems," *IEEE Trans. Signal Process.*, vol. 57, no. 12, pp. 4837–4851, Dec. 2009.

[5] C. Li, X. Wang, L. Yang, and W.-P. Zhu, "A joint source and relay power allocation scheme for a class of MIMO relay systems," *IEEE Trans. Signal Process.*, vol. 57, no. 12, pp. 4852–4860, Dec. 2009.

[6] Y. Huang, L. Yang, M. Bengtsson, and B. Ottersten, "A limited feedback joint precoding for amplify-and-forward relaying," *IEEE Trans. Signal Process.*, vol. 58, no. 3, pp. 1347–1357, Mar. 2010.

[7] O. Muñoz-Medina, J. Vidal, and A. Augustin, "Linear transceiver design in nonregenerative relays with channel state information," *IEEE Trans. Signal Process.*, vol. 55, no. 6, pp. 2593–2604, Jun. 2007.

[8] S. W. Peters and R. W. Heath, Jr, "Nonregenerative MIMO relaying with optimal transmit antenna selection," *IEEE Signal Process. Lett.*, vol. 15, pp. 421–424, 2008.

[9] S. Simoens, O. Muñoz-Medina, J. Vidal, and A. del Coso, "Compress-and-forward cooperative MIMO relaying with full channel state information," *IEEE Trans. Signal Process.*, vol. 58, no. 2, pp. 781–791, Feb. 2010.

[10] M. Yuksel and E. Erkip, "Multiple-antenna cooperative wireless systems: A diversity-multiplexing tradeoff perspective," *IEEE Trans. Inf. Theory*, vol. 53, no. 10, pp. 3371–3393, Oct. 2007.

[11] S. Simoens, O. Muñoz-Medina, J. Vidal, and A. del Coso, "On the Gaussian MIMO relay channel with full channel state information," *IEEE Trans. Signal Process.*, vol. 57, no. 9, pp. 3588–3599, Sep. 2009.
[12] E. C. Van Der Meulen, "Three-terminal communication channels," *Adv. Appl. Probab.*, vol. 3, pp. 120–154, 1971.
[13] T. M. Cover and A. A. El Gamal, "Capacity theorems for the relay channel," *IEEE Trans. Inf. Theory*, vol. 25, no. 5, pp. 572–584, Sep. 1979.
[14] B. Wang, J. Zhang, and A. Høst-Madsen, "On the capacity of MIMO relay channels," *IEEE Trans. Inf. Theory*, vol. 51, no. 1, pp. 29–43, Jan. 2005.
[15] A. Høst-Madsen and J. Zhang, "Capacity bounds and power allocation for wireless relay channels," *IEEE Trans. Inf. Theory*, vol. 51, no. 6, pp. 2020–2040, Jun. 2005.
[16] G. Kramer, M. Gastpar, and P. Gupta, "Cooperative strategies and capacity theorems for relay networks," *IEEE Trans. Inf. Theory*, vol. 51, no. 9, pp. 3037–3063, Sep. 2005.
[17] Z. Zhang and T. M. Duman, "Capacity-approaching turbo coding and iterative decoding for relay channels," *IEEE Trans. Commun.*, vol. 53, no. 11, pp. 1895–1905, Nov. 2005.
[18] Y. Liang, V. V. Veeravalli, and H. V. Poor, "Resource allocation for wireless fading relay channels: Max-min solution," *IEEE Trans. Inf. Theory*, vol. 53, no. 10, pp. 3432–3453, Oct. 2007.
[19] V. R. Cadambe and S. A. Jafar, "Degrees of freedom of wireless networks with relays, feedback, cooperation, and full duplex operation," *IEEE Trans. Inf. Theory*, vol. 55, no. 5, pp. 2334–2344, May 2009.
[20] W. T. Slingsby and J. P. McGeehan, "Antenna isolation measurements for on-frequency radio repeaters," in *Proc. 9th Int. Conf. Antennas Propag.*, Apr. 1995, vol. 1, pp. 239–243.
[21] H. Hamazumi, K. Imamura, N. Iai, K. Shibuya, and M. Sasaki, "A study of a loop interference canceller for the relay stations in an SFN for digital terrestrial broadcasting," in *Proc. IEEE Global Telecommun. Conf.*, Nov. 2000, vol. 1.
[22] C. R. Anderson, S. Krishnamoorthy, C. G. Ranson, T. J. Lemon, W. G. Newhall, T. Kummetz, and J. H. Reed, "Antenna isolation, wideband multipath propagation measurements, and interference mitigation for on-frequency repeaters," in *Proc. IEEE SoutheastCon*, Mar. 2004, pp. 110–114.
[23] K. M. Nasr, J. P. Cosmas, M. Bard, and J. Gledhill, "Performance of an echo canceller and channel estimator for on-channel repeaters in DVB-T/H networks," *IEEE Trans. Broadcasting*, vol. 53, no. 3, pp. 609–618, Sep. 2007.
[24] D. W. Bliss, P. A. Parker, and A. R. Margetts, "Simultaneous transmission and reception for improved wireless network performance," in *Proc. IEEE 14th Workshop on Statist. Signal Process.*, Aug. 2007.
[25] A. Hazmi, J. Rinne, and M. Renfors, "Diversity based DVB-T in-door repeater in slowly mobile loop interference environment," in *Proc. 10th Int. OFDM-Workshop*, Aug.–Sep. 2005.
[26] H. Ju, E. Oh, and D. Hong, "Improving efficiency of resource usage in two-hop full duplex relay systems based on resource sharing and interference cancellation," *IEEE Trans. Wireless Commun.*, vol. 8, no. 8, pp. 3933–3938, Aug. 2009.
[27] B. Chun, E.-R. Jeong, J. Joung, Y. Oh, and Y. H. Lee, "Pre-nulling for self-interference suppression in full-duplex relays," in *Proc. APSIPA Ann. Summit and Conf.*, Oct. 2009.
[28] P. Larsson and M. Prytz, "MIMO on-frequency repeater with self-interference cancellation and mitigation," in *Proc. IEEE 69th Veh. Technol. Conf.*, Apr. 2009.
[29] J. Sangiamwong, T. Asai, J. Hagiwara, Y. Okumura, and T. Ohya, "Joint multi-filter design for full-duplex MU-MIMO relaying," in *Proc. IEEE 69th Veh. Technol. Conf.*, Apr. 2009.
[30] Y. Y. Kang and J. H. Cho, "Capacity of MIMO wireless channel with full-duplex amplify-and-forward relay," in *Proc. IEEE 20th Int. Symp. Pers., Indoor and Mobile Radio Commun.*, Sep. 2009.
[31] J. Ma, G. Y. Li, J. Zhang, T. Kuze, and H. Iura, "A new coupling channel estimator for cross-talk cancellation at wireless relay stations," in *Proc. IEEE Global Commun. Conf.*, Dec. 2009.
[32] T. Riihonen, S. Werner, and R. Wichman, "Spatial loop interference suppression in full-duplex MIMO relays," in *Proc. 43rd Ann. Asilomar Conf. Signals, Syst. Comput.*, Nov. 2009.
[33] P. Persson, M. Coldrey, A. Wolfgang, and P. Bohlin, "Design and evaluation of a 2×2 MIMO repeater," in *Proc. 3rd Eur. Conf. Antennas Propag.*, Mar. 2009.
[34] K. Haneda, E. Kahra, S. Wyne, C. Icheln, and P. Vainikainen, "Measurement of loop-back interference channels for outdoor-to-indoor full-duplex radio relays," in *Proc. 4th Eur. Conf. Antennas Propag.*, Apr. 2010.

Taneli Riihonen (S'06) received the M.Sc. degree in communications engineering (with distinction) from Helsinki University of Technology, Finland, in February 2006. He was a student with the Graduate School in Electronics, Telecommunications and Automation (GETA) during 2006–2010.

During summer 2005, he was an intern at Nokia Research Center, Helsinki. Since fall 2005, he has been a researcher with the Department of Signal Processing and Acoustics, Aalto University School of Electrical Engineering (formerly known as Helsinki University of Technology) where he is completing the D.Sc. (Tech.) degree. His research activity is focused on physical-layer OFDM(A) and relaying techniques.

Stefan Werner (SM'07) received the M.Sc. degree in electrical engineering from the Royal Institute of Technology (KTH), Stockholm, Sweden, in 1998, and the D.Sc. (EE) degree (with honors) from the Signal Processing Laboratory, Smart and Novel Radios (SMARAD) Center of Excellence, Helsinki University of Technology (TKK), Espoo, Finland, in 2002.

He is currently an Academy Research Fellow with the Department of Signal Processing and Acoustics, Aalto University, Finland, where he is also appointed as a Docent. His research interests include adaptive signal processing, signal processing for communications, and statistical signal processing.

Dr. Werner is a member of the editorial board for the EURASIP *Signal Processing* journal.

Risto Wichman received the M.Sc. and D.Sc. (Tech) degrees in digital signal processing from Tampere University of Technology, Tampere, Finland, in 1990 and 1995, respectively.

From 1995 to 2001, he was with Nokia Research Center as a Senior Research Engineer. In 2002, he joined the Department of Signal Processing and Acoustics, Aalto University School of Electrical Engineering, where he has been a Professor since 2003. His major research interests include digital signal processing for applications in wireless communications.